Title
Intralaboratory repeatability of residual stress determined by the slitting method

Journal
Experimental Mechanics, 47

ISSN
0014-4851

Authors
Lee, M. J.
Hill, M. R.

Publication Date
2007-12-01

Peer reviewed

Intralaboratory Repeatability of Residual Stress Determined by the Slitting Method

Matthew J. Lee, Michael R. Hill*

Submitted to Experimental Mechanics, July, 2006

ABSTRACT

This paper presents repeated slitting method measurements of the residual stress versus depth profile through the thickness of identically prepared samples, which were made to assess repeatability of the method. Measurements were made in five 17.8 mm thick blocks cut from a single plate of 316L stainless steel which had been uniformly laser peened to induce a deep residual stress field. Typical slitting method techniques were employed with a single metallic foil strain gage on the back face of the coupon and incremental cutting by wire EDM. Measured residual stress profiles were analyzed to assess variability of residual stress as a function of depth from the surface. The average depth profile had a maximum value of –668 MPa at the peened surface. The maximum variability also occurred at the surface and had a standard deviation of 15 MPa and an absolute maximum deviation of 26 MPa. Since measured residual stress exceeded yield strength of the untreated plate, microhardness versus depth profiling and elastic-plastic finite element analysis were combined to bound measurement error from inelastic deformation.

Keywords: Slitting Method, Crack Compliance, Residual Stress, Repeatability, Laser Peening

1. INTRODUCTION

This paper describes the measurement of residual stress in five laser peened coupons using the slitting method (formerly called crack compliance). The purpose of the measurements is to quantify the intralaboratory repeatability of slitting on coupons with uniform residual stress. While the variation in residual stress due to intentional process variations in laser peening has been previously investigated [1, 2], no study has investigated the consistency of residual stress measured in identically prepared laser peened coupons. Further, there has been no formal study of the repeatability of the slitting method.

The slitting method for measuring residual stress was originally developed by Finnie and co-workers [3-7] and was recently reviewed by Prime [8]. Various forms of the slitting method have

been employed to measure residual stresses in a wide variety of materials (metal, glass, crystal, and plastic) and geometries (block, beam, plate, rod, tube, and ring) [9-17]. The specific slitting application addressed in this work is the determination of residual stress versus depth in a uniformly processed flat block of 316L stainless steel.

Laser peening was used to produce residual stress bearing samples for this study. Laser peening is a highly controlled, repeatable, spot-by-spot process [18-20]. The present work employed 316L stainless steel samples. Previous work on laser peened 316L by Peyre, et al [21] found significant levels of near-surface compressive residual stress (up to -500 MPa). The process also induced work-hardening and chemical modifications that increased corrosion resistance to a larger degree than did conventional shot peening. Other research (e.g., [1, 2, 12]) has shown that laser peening induces compressive residual stress to depths from the surface on the order of a few mm in a wide range of materials. In most published work, comparison of laser peened and conventionally shot peened samples has shown that laser peening produces deeper and higher magnitude residual stress [1] and longer fatigue life [22]. Laser peening was therefore highly desirable for the present study, due to its repeatability and the significant depth and magnitude of the residual stress profile imposed.

2. METHODS

Consistent stress samples

A set of residual stress bearing samples was prepared by uniformly laser peening one surface of a single large plate and cutting this plate into small blocks. The plate material was 316L stainless steel (composition in Table 1), having dimensions 19.0 mm thick, 102 mm wide, and 254 mm long (Figure 1). After receiving the material, the thickness was machined to 17.8 mm to provide a consistent thickness and surface quality. Laser peening was applied uniformly across

the full surface of one side of the plate (shaded region in Figure 1) using process parameters selected to provide a distribution of residual stress that would extend to significant depth below the treated surface.

Laser peening was carried out using a neodymium-doped, glass slab, flash lamp pumped laser. The basic system architecture was described by Dane, et al [23]. The residual stress imposed by laser peening in a given material and geometry depends on process coverage and laser pulse characteristics [1]. Coverage metrics include: laser spot size, measured at the treated surface; the number of layers of peening, where one layer consists of complete coverage of the subject area by raster of a sufficient number of individual spots; in-layer overlap, which reflects the percentage of spot size that two consecutive, neighboring spots overlap each other; and layer-to-layer offset, which reflects the spatial offset of one layer relative to the preceding layer. Laser pulse characteristics include irradiance, the power in the laser pulse divided by the laser spot area, and pulse duration, the duration of laser pulse. In the present work, we employed square laser spots with side length of approximately 3 mm and in-layer overlap of 3% (in the *y*-*z* plane of Figure 1). Four layers of peening were applied to the plate surface, with layer-to-layer offset of 25% of the spot size (along each axis of the *y*-*z* plane). Each laser pulse had a nominal irradiance of 10 GW/cm^2 and a pulse duration of 18 ns. To maximize consistent peening, the entire plate and all of the layers were peened on the same day.

After laser peening, ten blocks were cut from the plate (Figure 1), each measuring 17.8 mm thick, 50.8 mm wide, and 48.3 mm long. Of these the ten blocks, 1, 3, 4, 7, and 9 were used for slitting, block 10 was instrumented with a strain gage and used for thermal compensation during slitting, blocks 6 and 8 were used for other residual stress experiments, and block 5 was left as a

back-up coupon. Slitting was also carried out on block 2, and results of that measurement are discussed later.

Slitting method

The slitting method was used to determine residual stress through the thickness of each laser peened 316L block. Residual stress was obtained by measuring strain release occurring due to incremental extension of a slit into the depth of the block and solving for residual stress from measured strain. The specific stress computation procedure employed is described in detail in Lee and Hill [24], and a summary of the approach is provided here.

Stress computation

Stress computation assumed a polynomial basis for the stress versus depth profile, elastic superposition, and a linear system developed using finite element analysis. The residual stress as a function of depth $\sigma(x)$ was assumed to be described by a polynomial expansion of order m, having Legendre basis functions $P_j(x)$ and amplitudes A_j

$$\sigma(x) = \sum_{j=2}^{m} A_j P_j(x). \tag{1}$$

Legendre polynomials of order ≥ 2 were used because they have the property of satisfying stress equilibrium when integrated over the full sample thickness. Assuming elastic behavior, superposition can be employed to express strain released as a slit of depth a_i ($0 < a_i < t$) is cut through the block containing the stress of Equation (1) as

$$\varepsilon(a_i) = \sum_{j=2}^{m} C_{ij} A_j \,. \tag{2}$$

where C_{ij} is a linear system called the compliance matrix. Each element of the compliance matrix is the strain occurring for a slit of depth a_i when residual stress is given exactly by a particular basis function of the stress expansion P_j

$$C_{ij} = \varepsilon(a_i)\big|_{\sigma(x)=P_j(x)}. \tag{3}$$

Compliance matrix elements are typically computed using finite element analysis, but the present work makes use of recent results that provide the compliance matrix for a flat block in closed form (Lee and Hill [24]). The pseudoinverse of the compliance matrix is used to compute the amplitudes of the stress expansion A_j from measured strain data. Adopting a matrix notation for Equation (2), with rows in [C] representing the set of incremental slit depths a_i and columns representing the set of polynomial basis functions P_j, a least squares inversion of Equation (2) gives a vector of basis amplitudes $\{A\}$ from a vector of measured strain versus depth data $\{\varepsilon_{meas}\}$

$$\{A\} = [(C^{\mathrm{T}}C)^{-1}C^{\mathrm{T}}]\{\varepsilon_{meas}\}. \tag{4}$$

Inserting these basis amplitudes into Equation (1) produced the residual stress profile. This analysis was repeated for a range of assumed Legendre series order, m, and the series order of the final result was determined by minimizing stress error, as described by Hill and Lin [16].

Slitting procedures

The slitting procedures were to instrument the coupon with a single strain gage and to slit through the specimen thickness while measuring released strain at specified depth increments.

Each block was instrumented with a strain gage having gage length of 0.79 mm, gage width of 0.81 mm, nominal resistance of 350Ω, and a gage factor 2.06. The strain gage was precisely

placed opposite the cut face and on the slit plane (i.e., as in Figure 2 with $s = 0$) and was oriented to measure strain perpendicular to the slit direction (along the y-direction of Figure 2). Because the slitting was performed by wire EDM with the coupon submerged in water, the strain gages were waterproofed with a silicone-based adhesive/sealant to prevent contamination and electrical conductance while submerged.

The wire EDM was fitted with 0.254 mm wire and had de-ionized water in the basin. Finish-pass cutting parameters were used to minimize the amount of mechanical strain induced by the EDM. A cutting direction consistent with the gage placement and finite element modeling was ensured by aligning the block with the EDM coordinate axes. To make sure each slit depth was achieved, the EDM was set to dwell for 7.5 seconds at each depth. After dwelling, the EDM was halted so that stray voltages from the wire did not affect measured strains.

Strains were measured by a commercial Wheatstone bridge strain indicator. The accuracy of the strain measurements was taken to be ± 3 (με), and was considered in the error analysis [16]. To minimize thermal strain, block 10 was identically gaged, placed in the EDM basin, and wired as a half-bridge thermal compensator.

Adjustments for errors due to geometrical imperfections in the experiment were made by methods outlined earlier [1, 16]. One necessary adjustment is a correction for the actual slit depth being different than the intended slit depth, where the actual slit depth was determined following slitting using digital photogrammetry and used to adjust all slit depths [1].

The intended final slit depth was 17.27 mm. The slitting increments were 0.127 mm for the first eight depths, 0.254 mm for the next ten depths, followed by 0.508 mm for seventeen depths, and then 1.016 mm for the remaining depths.

Data analysis

To quantify the variability in stress, the standard deviation and the maximum point wise error in stress were calculated for the five blocks. The standard deviation was calculated as [25]

$$\chi(a_i) = \sqrt{\frac{1}{(N-1)}\sum_{k=1}^{N}\left[\sigma_k(a_i) - \overline{\sigma}(a_i)\right]} \tag{5}$$

where χ is the standard deviation, a_i is the average slit depth at increment i, N is the number of coupons (5), k represents each coupon (1 through 5 representing coupon numbers 1, 3, 4, 7, 9), and $\overline{\sigma}(a_i)$ is the average stress at a given depth

$$\overline{\sigma}(a_i) = \frac{1}{N}\sum_{k=1}^{N}\sigma_k(a_i). \tag{6}$$

The maximum point-wise stress error at a given depth, $e_{\max}(x)$, is the maximum departure from the average stress over all coupons, k

$$e_{\max}(a_i) = \max_{k=1,5}\left[\left|\sigma_k(a_i) - \overline{\sigma}(a_i)\right|\right]. \tag{7}$$

3. RESULTS

Strain measurements and fits for the five slitting coupons are shown in Figure 3. Block 2 results shown in Figure 3 will be described later. Actual final slit depth ranged from 17.19 mm to 17.21 mm (intended to be 17.27 mm). For each coupon, the last measured strain data point was omitted from stress computation because the measured strains departed abruptly from the trend for shallower depths (Figure 3). This has been observed previously in the literature and results from the decreased rigidity of the uncut ligament at large slit depth. Data reduction, error analysis and order selection [16] provided orders 4 or 7 for the stress polynomial in each coupon (Table 2). The resulting stresses (Figure 4) were nearly identical for all coupons. The strain fits provided by the stress computation (Figure 3) had very small lack-of-fit errors for each block,

which resulted in small stress uncertainties. Error bars on the individual stress profiles of Figure 4 are omitted for clarity, but maximum stress uncertainty occurred for block 7, being 35 MPa at the surface and having a root mean square (RMS) uncertainly, computed over all depths, of 12 MPa. The average stress versus depth profile had a maximum compressive residual stress of -668 MPa near the surface, and a stress zero-crossing at 2.9 mm into the depth. Laser peening induced stress reached down to about 9 mm, where the stress becomes linear and consists of bending and axial stresses arising for equilibrium.

Plotted on the right-hand axis of Figure 4 are standard deviation (Equation (5)) and the maximum point-wise error (Equation (7)) for the stress versus depth profiles. The resulting maximum standard deviation and point-wise error were 15 MPa and 26 MPa, respectively. Both of these maximum errors were near the surface where small slit depths produce small magnitude strains at the remote back-face gage.

4. DISCUSSION

The objective of this study was to investigate the intralaboratory repeatability of the slitting method. The resulting residual stresses had the most variability near the start of the slit, where the standard deviation was 15 MPa. At greater depths, variability was significantly less. The standard deviation of 15 MPa near the surface translates to 2% when normalized by the maximum measured stress at that location.

Outlying data

Block 2 was also measured during this work, but was excluded from the repeatability analysis based on Chauvenet's criterion. Stress versus depth results for block 2 were computed as for other samples, but these data departed significantly from results for the other five blocks. In order to assess whether these data were an outlier, Chauvenet's criterion [26] was used. The

criterion assumes a normal distribution for the population of measured data, determines the value of the standard normal variate for a suspect data point, and computes the probability that a result would fall farther from the population mean than the suspect point. In order to apply the criterion for slitting data, the analysis was preformed for each depth of cut and results were averaged for all depths. At each depth, the standard normal variate for a suspect data point, $z_{sus}(a_i)$, was computed from the suspect stress, $\sigma_{sus}(a_i)$, the average stress (as in Equation (6), but with $N = 6$ and including results for block 2), and the standard deviation $\chi(a_i)$ (as in Equation (5), but with $N = 6$ and including results for block 2)

$$z_{sus}(a_i) = \frac{\sigma_{sus}(a_i) - \overline{\sigma}(a_i)}{\chi(a_i)}. \tag{8}$$

The average of $z_{sus}(a_i)$ was then computed over all $n = 39$ slit depths at which stress was computed

$$z_{sus,ave} = \frac{1}{n}\sum_{i=1}^{n} z_{sus}(a_i) \tag{9}$$

for a given suspect coupon. The probability $P(z > z_{sus})$ was then computed from a standard Normal distribution probability table. Chauvenet's criterion calls for rejection of a data point as an outlier if the expected number of measurements at least as far from the mean as the suspect measurement is less than 0.5

$$0.5 \geq N\,P(z > z_{sus}). \tag{10}$$

Assessing block 2 as a suspect data point, and using $z_{sus,ave}$ in place of z_{sus} because we are investigating an entire stress profile, we find $NP(z > z_{sus,ave}) = 0.005$, which easily meets Chauvenet's criterion. Block 2 was therefore treated as an outlier from the other 5 blocks and not

included in the repeatability analysis. For comparison, the next smallest $NP(z > z_{sus,ave})$ was 1.3 for block 7.

Magnitudes of residual stress and yield strength

Stated yield strength of the 316L plate used in this study (308.7 MPa) is significantly smaller than the measured near-surface residual stress magnitude (-668 MPa). While strain hardening from laser peening likely increased near-surface yield strength in the peened plate, high measured residual stresses are of concern because the data reduction for slitting assumes elastic deformation. This motivated an investigation of the distribution of near-surface yield strength in the peened plate and an analysis of the effect of elastic-plastic behavior on residual stress measured by slitting.

Microhardness data were collected versus depth from the peened surface on a prepared block from this study. Earlier work has shown that laser peening increases microhardness of a material at the peened surface through cold work, with the effect decreasing as a function of depth from the treated surface [27]. A Leitz Wetzlar Metallux 3 Vickers Microhardness Tester was used to get four microhardness versus depth profiles to a maximum depth of 11 mm, using 100 grams of force and a dwell time of 10 seconds (Figure 5). These 4 depth profiles were then interpolated at common depths and used to determine an average microhardness profile as a function of depth from the peened surface (Figure 5).

The average microhardness profile was used with a recently published correlation to estimate yield strength as a function for depth from the peened surface. Nobre [28] found that yield strength at a given depth from a shot peened surface could be determined from hardness increase and pre-treatment yield strength

$$S_y(x) = S_{y,0}\left(1 + \gamma \frac{\Delta H(x)}{H_{y,0}}\right) \tag{11}$$

where $S_y(x)$ is the local yield strength at depth x, $S_{y,0}$ is the bulk pre-treatment yield strength, γ is an empirical constant, $\Delta H(x)$ is the local increase of hardness over bulk, and $H_{y,0}$ is the hardness of the bulk material. The pre-treatment material constants were $S_{y,0}$ = 308.7 MPa and $H_{y,0}$ = 298.0. Nobre found the empirical constant to be γ = 2.8 for carbon steels over a wide range of hardness, yield strength, and strain hardening, and this value was used here to estimate the behavior of 316L, which has flow properties within the range of those materials investigated by Nobre [28]. A plot of local yield strength versus depth overlaid with a plot of the absolute value the residual stresses versus depth (Figure 6) suggests that the residual stress magnitude exceeded local yield strength over a very small region at the peened surface (depths ≤ 0.35 mm).

Elastic-plastic analysis

In order to understand error (bias) that may have arisen in the data reduction due to elastic-plastic behavior, an elastic-plastic simulation was run to provide an error bound. The simulation took as input the average stresses, $\overline{\sigma}(x)$, from the linear-elastic residual stress data reduction and simulated the slitting process assuming elastic-plastic material behavior. The simulation output provided a strain versus depth record that was subsequently used with the (elastic) residual stress data reduction for slitting. The difference between residual stress so computed and $\overline{\sigma}(x)$ provides an error bound due to elastic plastic behavior.

The elastic plastic simulation required a stress-strain curve, which was assumed to be given by a Ramberg-Osgood flow curve [29]

$$\frac{\varepsilon}{\varepsilon_o} = \frac{\sigma}{\sigma_o} + \alpha\left(\frac{\sigma}{\sigma_o}\right)^n \tag{12}$$

where σ_o is a reference stress (0.2% offset yield stress, when $\alpha = 1$), $\varepsilon_o = \sigma_o/E$ is a reference strain, α is taken to be 1, and n is the work-hardening exponent. The values assumed for reference stress and Young's Modulus were $\sigma_o = S_y$= 308.7 MPa and E = 206.9 GPa. The work-hardening exponent was calculated from the ratio of ultimate tensile strength, S_u, to S_y and non-linear root finding using

$$R = \frac{S_u}{S_y} = \left(\frac{1}{0.002n}\right)^{1/n} \Big/ \exp^{1/n} \tag{13}$$

which is based on a constancy of volume assumption during plastic deformation [29]. Taking S_u = 600 MPa gives n = 5.33.

In the present case, the laser peened block exhibited a non-uniform state of strain hardening, and this was included in the simulation. For a given material point at depth x from the surface (Figure 2), a hardening state was defined by using the material flow curve and a simplified fit to the local yield strength $S_{y,0}(x)$ data (Figure 6). At each depth, a value of plastic strain was defined to quantify hardening by solving Equation (12) for ε given $\sigma = S_{y,0}(x)$, then subtracting the elastic strain σ/E. The finite element code [30] allowed definition of the initial yield surface size by stating initial plastic strain at each point in the model, which accounted for the spatially dependent strain hardening from laser peening.

Given the elastic-plastic material model, the simulation employed normal procedures followed when determining compliance matrices for slitting [24], with the exception of loading. While slitting simulation for elastic material normally employs tractions, the present situation required imposing $\overline{\sigma}(x)$ as an initial stress. The analysis proceeded by first imposing the residual

stress, then taking an equilibrium step to define a reference mechanical state. Slitting was then simulated by altering boundary conditions such that a slit was extended incrementally though the model in a series of analysis steps (each step corresponding to a single slit depth). At each step, deformation from the reference state was then used to compute strain occurring at the strain gage location, as would normally be done when simulating slitting [24]. Combining simulation results for a series of analysis steps that extended the slit through all slit depths provided strain versus depth data, which was used with the previously defined (elastic) residual stress data reduction to determine residual stress. The resulting elastic-plastic residual stress profile $\sigma_{ep}(x)$ differs somewhat from $\overline{\sigma}(x)$ (Figure 7), with the largest differences at the peened surface.

For equal stress, elastic strains are smaller than elastic-plastic strains. Strains measured in the experiments were apparently elastic-plastic strains, larger than would have occurred under elastic conditions. The residual stresses computed from these larger strains are therefore an overestimate of the true residual stress magnitude. Since this overestimate of residual stress was used as the input into the elastic-plastic model and used to derive an error bound, the errors in Figure 7 are conservative. The maximum error due to elastic-plastic effects was 69 MPa and occurred at the peened surface.

5. CONCLUSION

The intralaboratory repeatability of the slitting method was assessed by measurement of residual stress contained in five block coupons that were identically prepared. The five block coupons were prepared so that all contained practically identical distributions of residual stress as a function of depth from one surface. Each block was cut from a larger 316L stainless steel plate that had been annealed and then uniformly treated with laser peening. Parameters for laser peening were selected to provide a distribution of residual stress that was highly compressive at

the treated surface and had a large depth of compressive residual stress. The slitting method was then employed, following typical procedures, to determine the profile of residual stress as a function of depth from the treated surface in each of the five block coupons. The average of all five depth profiles had a maximum value of -668 MPa at the treated surface and a zero crossing 2.9 mm below the treated surface. Variability of residual stress as a function of depth from the surface among the five coupons was largest near the treated surface, where the residual stress determined had standard deviation of 15 MPa and absolute maximum deviation of 26 MPa.

6. REFERENCES

[1] J. E. Rankin, M. R. Hill and L. A. Hackel, 2003, "The effects of process variations on residual stress in laser peened 7049 T73 aluminum alloy," Mater. Sci. Eng. A, **349**(1-2) pp. 279-291.

[2] A. T. Dewald, J. E. Rankin, M. R. Hill, M. J. Lee and H.-L. Chen, 2004, "Assessment of tensile residual stress mititagion in alloy 22 welds due to laser peening," J. Eng. Mater. Technol., **126**(4) pp. 465-473.

[3] W. Cheng, I. Finnie and O. Vardar, 1991, "Measurement of residual stresses near the surface using the crack compliance method," J. Eng. Mater. Technol., **113**(2) pp. 199-204.

[4] W. Cheng and I. Finnie, 1985, "A method for measurement of axisymmetric axial residual stress in circumferentially welded thin walled cylinders," J. Eng. Mater. Technol., **107**(3) pp. 181-185.

[5] S. Vaidyanathan and I. Finnie, 1971, "Determination of residual stress from stress intensity factor measurements," Appl. Mech. Rev., **52**(2) pp. 75-96.

[6] I. Finnie and W. Cheng, 1996, "Residual stress measurement by the introduction of slots or cracks," Localized Damage IV Computer Aided Assessment and Control of Localized Damage - Proceedings of the International Conference 1996. Computational Mechanics Inc, Billerica, MA, USA., pp. 37-51.

[7] I. Finnie and W. Cheng, 2002, "A summary of past contributions on residual stresses," Mater. Sci. Forum, (Vol.) 404-407, pp. 509-514.

[8] M. Prime, 1999, "Residual stress measurement by successive extension of a slot: the crack compliance method," Appl. Mech. Rev., **52**(2) p. 75.

[9] C. C. Aydiner, E. Ustundag, M. B. Prime and A. Peker, 2003, "Modeling and measurement of residual stresses in a bulk metallic glass plate," J. Non-Cryst. Solids, **316**(1) pp. 82-95.

[10] P. S. Midha and G. F. Modlen, 1976, "Residual stress relief in cold-extruded rod," Met. Technol., **3**(11) pp. 529-533.

[11] C. S. Cook, "Straightening operations and residual stresses in tubing," Publ by ASM Int, Metals Park, OH, USA, pp. 61-68.

[12] J. E. Rankin and M. R. Hill, 2003, "Measurement of thickness-average residual stress near the edge of a thin laser peened strip," J. Eng. Mater. Technol., **125**(3) pp. 283-293.

[13] M. B. Prime and M. R. Hill, 2002, "Residual stress, stress relief, and inhomogeneity in aluminum plate," Scripta Mater., **46**(1) pp. 77-82.

[14] M. B. Prime, V. C. Prantil, P. Rangaswamy and F. P. Garcia, 2000, "Residual stress measurement and prediction in a hardened steel ring," Mater. Sci. Forum, **347** pp. 223-228.

[15] D. Nowell, S. Tochilin and D. A. Hills, 2000, "Measurement of residual stresses in beams and plates using the crack compliance technique," J. Strain Anal. Eng. Des., **35**(4) pp. 277-285.

[16] M. R. Hill and W. Y. Lin, 2002, "Residual stress measurement in a ceramic-metallic graded material," J. Eng. Mater. Technol., **124**(2) pp. 185-191.

[17] A. T. DeWald, J. E. Rankin, M. R. Hill and K. I. Schaffers, 2004, "An improved cutting plan for removing laser amplifier slabs from Yb:S-FAP single crystals using residual stress measurement and finite element modeling," J. Cryst. Growth, **265**(3-4) pp. 627-641.

[18] C. B. Dane, L. A. Hackel, J. Daly and J. Harrisson, Laser peening of metals - enabling laser technology," High-Press. Mater. Res. Mater., **499 1998. MRS**(Warrendale, PA,) pp. 73-85.

[19] G. Hammersley, 1999, "Lasershot peening comes out of the lab," Mater. World, **7**(5) pp. 281-282.

[20] L. Hackel, 2003, "Laser Peening and Laser Peenforming: New Tools for Inducing Surface Stress," Light Met. Age, **61**(11-12 December) pp. 30-31.

[21] P. Peyre, X. Scherpereel, L. Berthe, C. Carboni, R. Fabbro, G. Beranger and C. Lemaitre, 2000, "Surface modifications induced in 316L steel by laser peening and shot-peening. Influence on pitting corrosion resistance," Mater. Sci. Eng. A, **280**(2) pp. 294-302.

[22] P. Peyre, R. Fabbro, P. Merrien and H. P. Lieurade, 1996, "Laser Shock Processing of Aluminium Alloys - Application to High Cycle Fatigue Behaviour," Mater. Sci. Eng. A, **210**(1-2) pp. 102-113.

[23] C. B. Dane, L. E. Zapata, W. A. Neuman, M. A. Norton and L. A. Hackel, 1995, "Design and operation of a 150 W near diffraction-limited laser amplifier with SBS wavefront correction," IEEE J. Quantum Electron., **31**(1) pp. 148-163.

[24] M. J. Lee and M. R. Hill, 2005, "Effect of strain gage length when determining residual stress by slitting," Accepted for publication in J. Eng. Mater. Technol., July 2006

[25] P. R. Bevington and D. K. Robinson, 1992, *Data reduction and error analysis for the physical sciences*, second ed, McGraw-Hill, Inc, New York.

[26] J. R. Taylor, 1982, *An Introduction to Error Analysis: The Study of Uncertainties in Physical Measurements*, first ed, University Science Books, Mill Valley, CA, pp. 142-145.

[27] I. Yakimets, C. Richard, G. Beranger and P. Peyre, 2004, "Laser peening processing effect on mechanical and tribological properties of rolling steel 100Cr6," Wear, **256**(3-4) pp. 311-320.

[28] J. P. Nobre, A. M. Dias and M. Kornmeier, 2004, "An empirical methodology to estimate a local yield stress in work-hardened surface layers," Exp. Mech., **44**(1) pp. 76-84.

[29] M. T. Kirk and Y.-Y. Wang, 1995, "Wide range CTOD estimation formulae for SE(B) specimens," ASTM Special Technical Publication. n 1256, Conshohocken, PA, USA, pp. 126-141.

[30] ABAQUS, version 6, Hibbitt, Karlsson, and Sorensen, Inc, Pawtucket, RI, 2003.

7. TABLES

C	Mn	P	S	Si	Ni	Cr	Mo	Co	Cu	N
0.019	1.68	0.03	0.005	0.4	10.14	16.25	2.08	0.23	0.37	0.062

Table 1: 316L Steel chemical composition (wt. percent)

Coupon #	1	3	4	7	9
Order Selected	4	7	4	4	4

Table 2: Order selection for slitting coupons

8. FIGURES

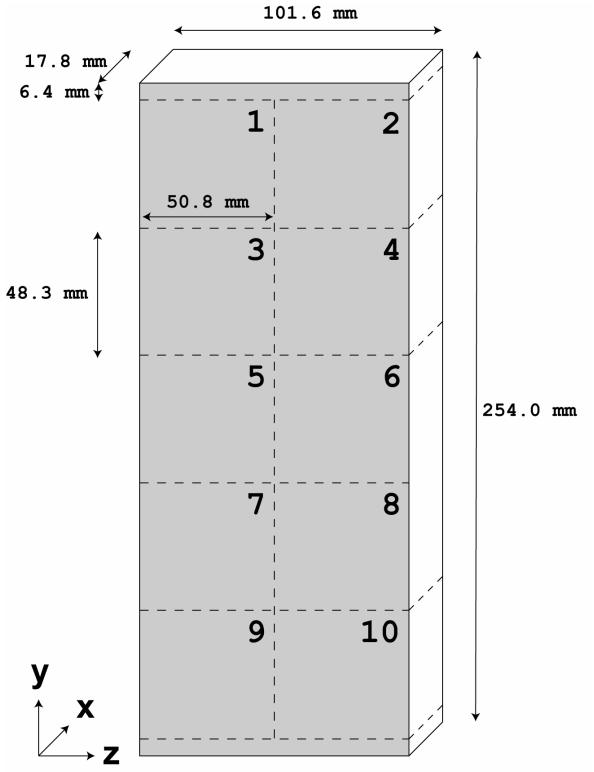

Figure 1: Coupon layout in laser peened 316L plate (uniformly treated surface shaded)

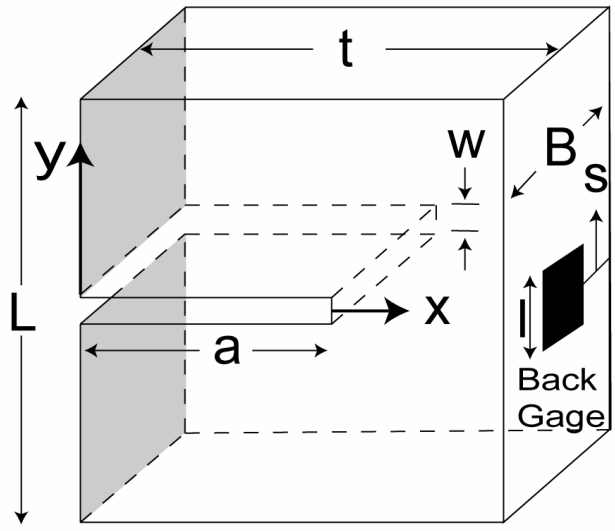

Figure 2: Block geometry variables: thickness of the part in the slitting direction t, slit depth a, slit width w, length L, gage length l, depth B, and distance between the center of the gage and center of the slit s. Shaded region represents the laser peened surface.

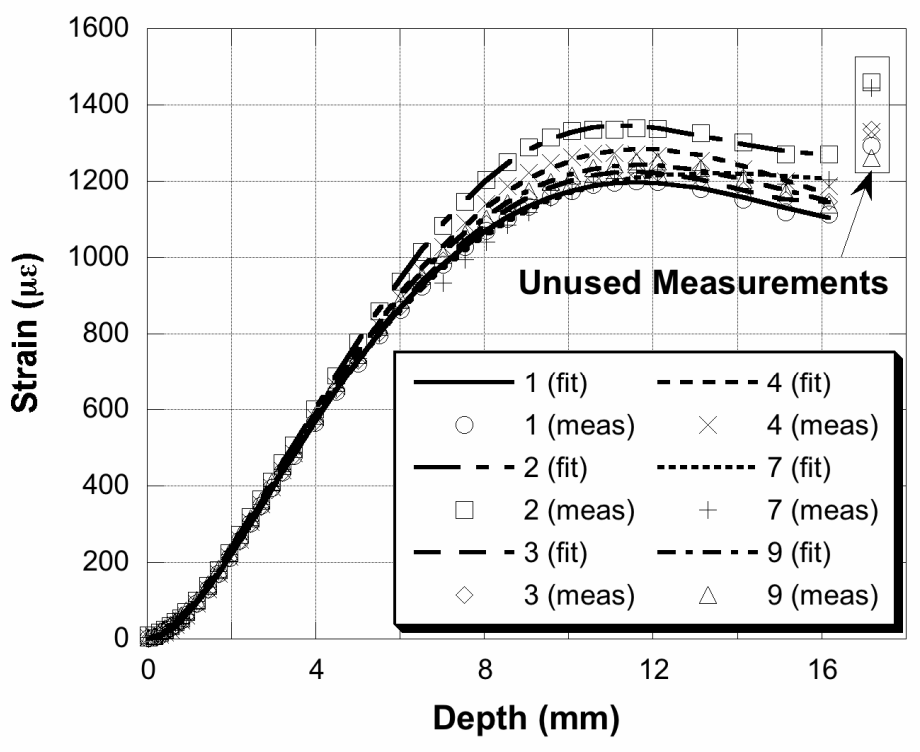

Figure 3: Measured strain data and strain fits for all coupons

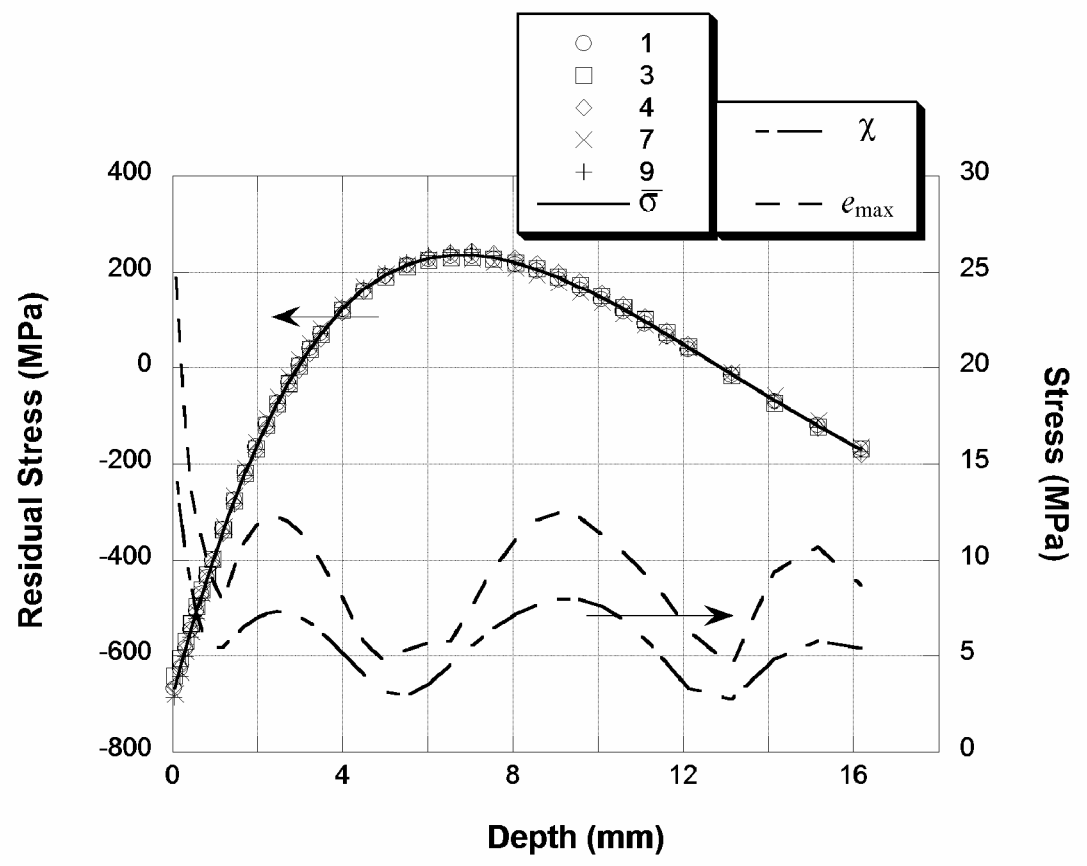

Figure 4: Residual stress for all coupons, average stress, and standard and maximum deviations

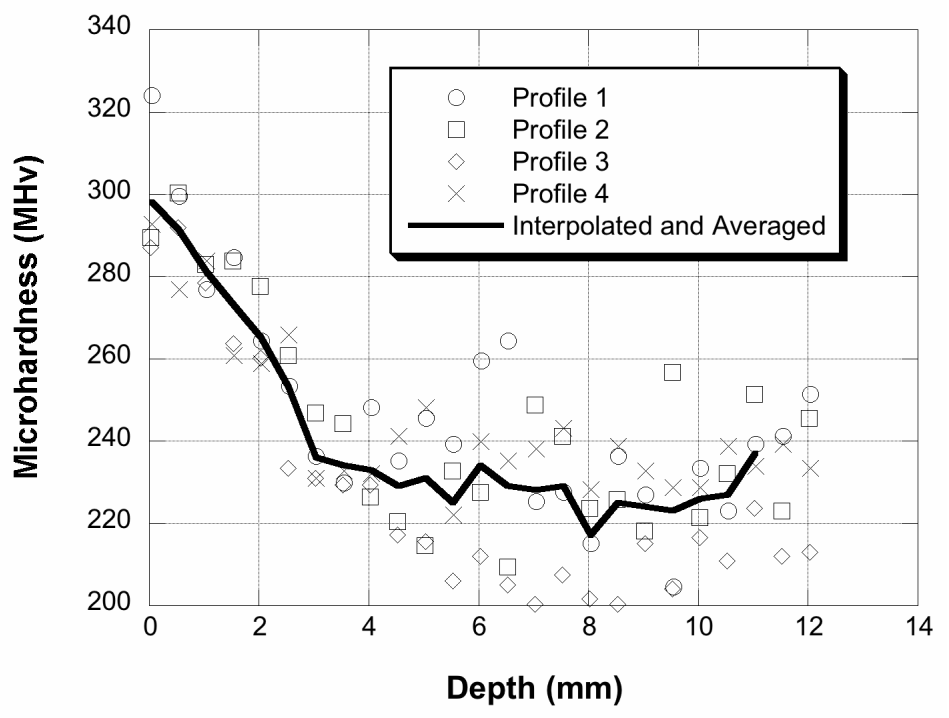

Figure 5: Microhardness profiles with interpolated and averaged profile

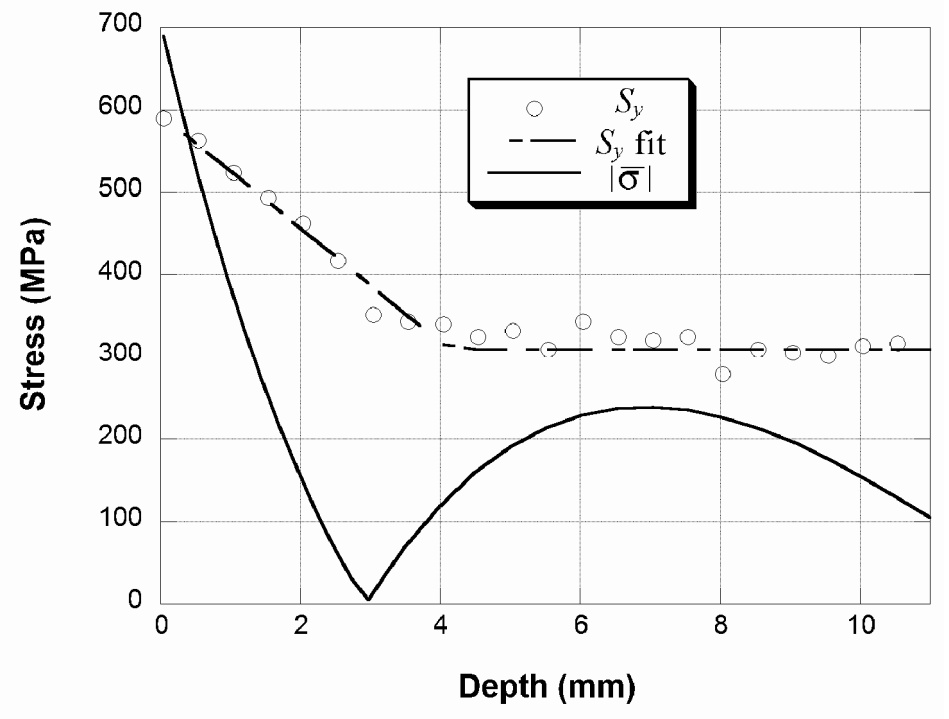

Figure 6: Yield strength and absolute value of average residual stress vs depth

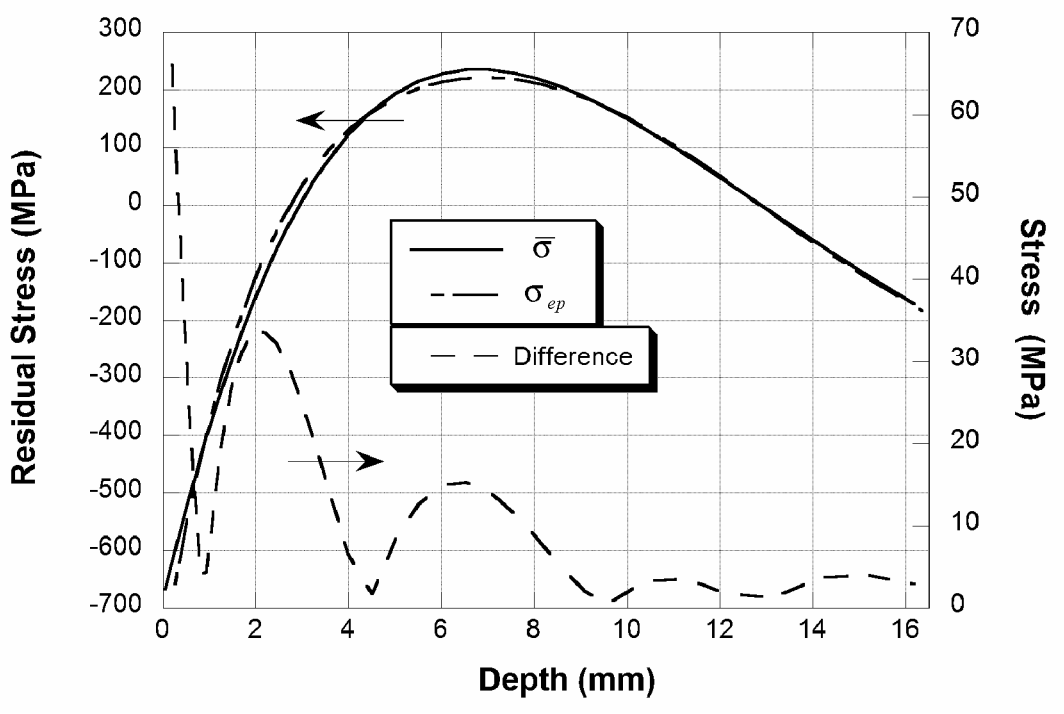

Figure 7: Average residual stress determined using elastic data reduction and residual stress resulting from elastic-plastic analysis